# Correlation of kinetic edge data with type-I and mitigated ELMs at ASDEX Upgrade

S.K. Rathgeber, L. Barrera, G. Birkenmeier, R. Fischer, W. Suttrop
and the ASDEX Upgrade Team
*Max-Planck-Institut für Plasmaphysik, EURATOM Association,*
*Boltzmannstraße 2, 85748 Garching, Germany*

**Introduction.** Mitigation of type-I Edge Localized Modes (ELMs) is likely required for ITER operation in order to reduce the heat flux on the divertor plates. In present day machines, non-axisymmetric Magnetic Perturbation (MP) fields are successfully applied to achieve H-mode discharges without or with small ELMs and appropriate confinement properties [1]. However, the underlying mechanism is not yet understood and detailed investigations on the plasma in the presence of MPs are necessary to assess the possibility of ELM control with MPs at ITER.

Since ELMs are assumed to be driven by large edge pressure gradients, this contribution focuses on the relation between kinetic edge data, occurring ELM type and MP-coil configuration at ASDEX Upgrade. A valuable tool for this study is provided by Integrated Data Analysis (IDA) [2] which has recently been improved by a model for the Electron Cyclotron Emission (ECE) enabling the reconstruction of accurate edge electron temperature profiles [3].

It is shown that mitigated ELMs generally — with and without MPs — occur in regimes with smaller pedestal top electron temperatures and edge electron pressure gradients than type-I ELMs, while with MPs there exists an additional small ELM regime in the high temperature range at reduced electron pressure gradient. We present results indicating that this profile flattening is not a consequence of field line ergodization but caused by a shifted stability limit.

**Integrated data analysis.** The edge kinetic profiles were estimated by means of IDA which combines the data of different complementary diagnostics for joint analysis of electron density and temperature in the framework of Bayesian probability theory [2]. Standard analysis, thereby, applies the lithium beam emission and interferometry diagnostic for the density and ECE data for the temperature reconstruction. Unlike previous straight forward ECE analysis of identifying the electron temperature with the radiation temperature at the cold resonance position of the measured frequency, we made use of the newly developed Electron Cyclotron Forward Modelling (ECFM) [3]. With this method we achieved accurate electron temperature profiles and gradients also in the optically thin and steep edge region by calculating the broadened emission and absorption profiles and solving the radiation transport equation.

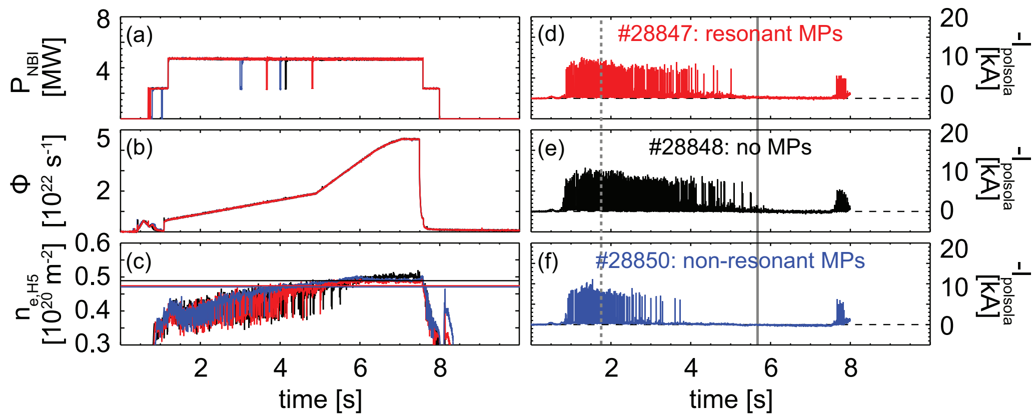


Figure 1: *Time traces of the NBI heating power (a), the gas puff (b), the line-averaged edge density (c) and the divertor current signals (d,e,f) of discharge #28847 with resonant MPs (red), #28848 without MPs (black) and #28850 with non-resonant MPs (blue); the vertical grey lines indicate the time points of the following profiles.*

**Discharge description.** Based on these reliable results, we performed a thorough investigation on the edge kinetic parameters in several discharges with varied MP-coil configuration, heating power and gas puff exhibiting regimes with both types of ELMs. Figure 1 shows an example of a triple of identical discharges but different MP-coil settings. They exhibited a medium heating power (a) of $P_{\mathrm{NBI}} = 4.9\,\mathrm{MW}$ and a large variation in gas puff (b) enabling phases with type-I ELMs only and small ELMs only in all three discharges. From the divertor current signal (d,e,f) it can be seen that complete type-I ELM suppression was achieved the fastest with non-resonant MPs (blue), but at the same density (c) as with resonant MPs (red). In the reference discharge without MPs (black) ELM mitigation was achieved last and the density threshold was slightly higher.

**Edge kinetic profiles.** For two time points (marked by the grey lines in Fig. 1) of these three discharges, the edge kinetic profiles just before an ELM crash are depicted in Fig. 2. The dashed lines illustrate the profiles at an early time point where type-I ELMs have still been present. The solid lines depict profiles of phases with small ELMs only. For the latter, also the ECE data (crosses) used for the electron temperature reconstruction and the modelled radiation temperature (pluses) given by ECFM are plotted in (a,e,i). Their good match inside $\rho_{\mathrm{pol}} \approx 1.02$ demonstrates that the presented electron temperature profiles were able to reproduce the measurement correctly. This can also be seen from the residuals in (b,f,j).

The comparison of the three columns shows that the profiles were very similar with resonant, non-resonant and without MPs. The profiles for the two time points of course differed due to the variation in gas puff. As a consequence of the strong deuterium fuelling at $t \approx 5.8$s, the electron density increased, the electron temperature was reduced, the edge pressure gradient slightly flattened and the type-I ELMs disappeared.

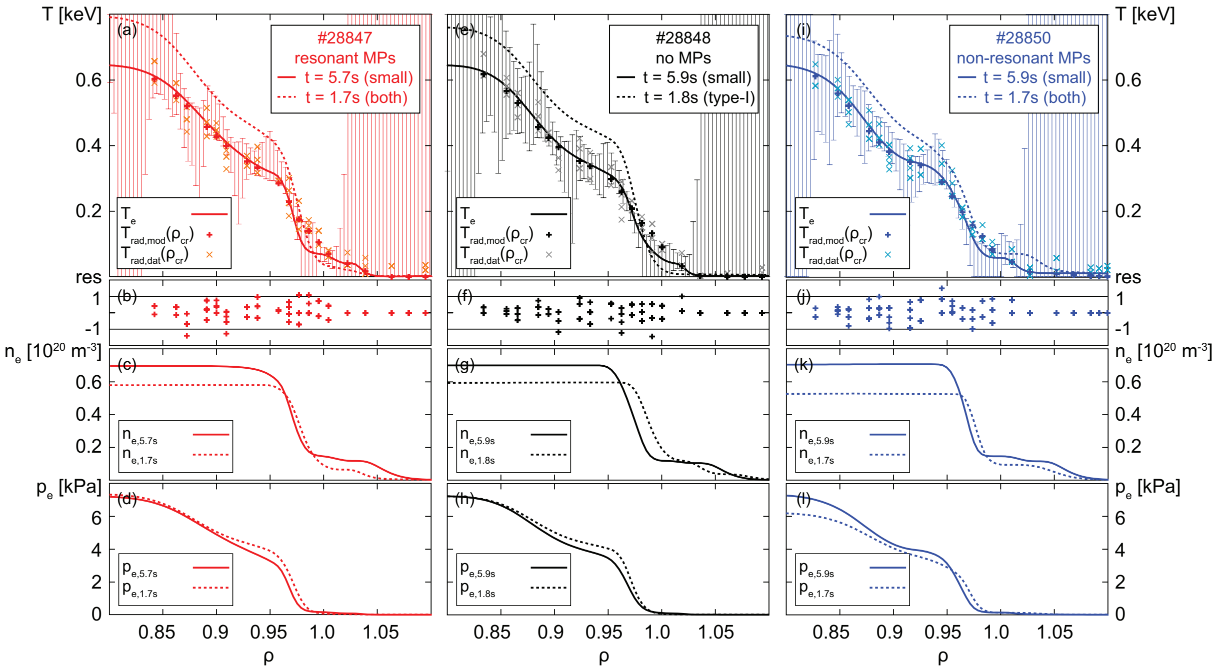


Figure 2: *Edge profiles of $T_e$ (a,e,i), $n_e$ (c,g,k) and $p_e$ (d,h,l) for discharge #28847 (left), #28848 (middle) and #28850 (right) at $t \approx 1.8$ s (dashed) and $t \approx 5.8$ s (solid); additionally shown are the modelled (pluses) and measured (crosses) $T_{rad}$ values at the positions of their cold resonance (a,e,i) and their residuals (b,f,j) at $t \approx 5.8$ s.*

**Correlation of edge kinetic data and ELM type.** The relation of the appearance of small or type-I ELMs to the edge kinetic data in general is demonstrated in Fig. 3 where the maximum edge pressure gradient before the ELM crash is plotted against the pedestal top electron temperature for the three presented discharges together with the data of several other experiments with different heating power and gas puff. Here, it is only distinguished between cases with (red) and without (black) MPs, since no significant difference between resonant and non-resonant MPs has been found. The different symbols mark the phases with type-I ELMs only (filled squares), small ELMs only (crosses) and both types of ELMs (empty squares).

The graph reveals the dominance of small ELMs in the low temperature regime with $T_{e,pedtop} \lesssim 350\,\mathrm{eV}$ — which is consistent with the findings in [4] — and a rather low upper threshold for the edge pressure gradient which strongly depended on the temperature. In this regime, the edge kinetic data were similar with and without MPs.

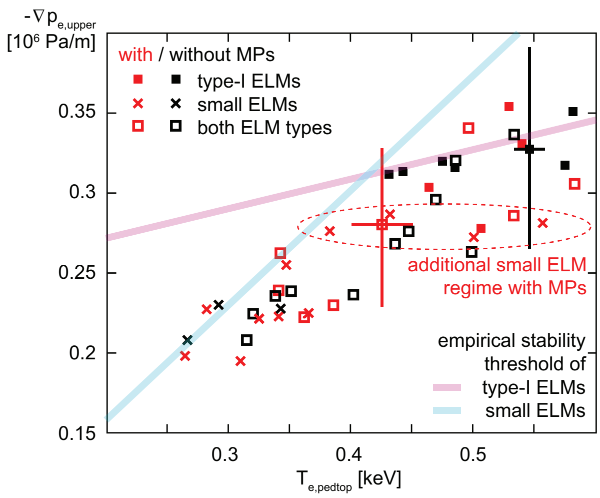


Figure 3: *Upper edge pressure gradient versus pedestal top temperature for various discharges with (red) and without (black) MPs; the different symbols indicate the ELM type; additionally plotted are lines to guide the eye.*

The high temperature regime with $T_{\mathrm{e,pedtop}} \gtrsim 400\,\mathrm{eV}$, on the contrary, was dominated by type-I ELMs which occurred at a significantly higher edge pressure gradient with a threshold not or only slightly varying with temperature. However, in the presence of MPs an additional regime with small ELMs occurring at reduced pressure gradients has been observed in this temperature range.

**MP-coil current threshold.** Another set of discharges with slow ramp-ups of the MP-coil current has been performed to study the current threshold at the onset of ELM mitigation under various conditions. According to the hypothesis that ELM mitigation with MPs is caused by pressure gradient degradation below the ballooning limit as a result of field line ergodization, the heat diffusivity $\chi_{\mathrm{eff}}$ should increase monotonically with the strength of the perturbation, i.e. with the MP-coil current. However, such a behaviour has not been observed as can be seen in Fig. 4 where the heat diffusivity — which is calculated from the electron kinetic data according to $\frac{P_{\mathrm{LOSS}}}{2A_{\mathrm{sep}}} = \frac{1}{2}(q_{\mathrm{e}} + q_{\mathrm{i}}) \approx -\chi_{\mathrm{eff}} n_{\mathrm{e}} \nabla T_{\mathrm{e}}$ — at the onset of ELM mitigation (crosses) is plotted against the required MP-coil current. Additionally shown as shaded squares are the corresponding values just before the MP onset which indicate that the heat diffusivity did not generally increase after switching on the MPs.

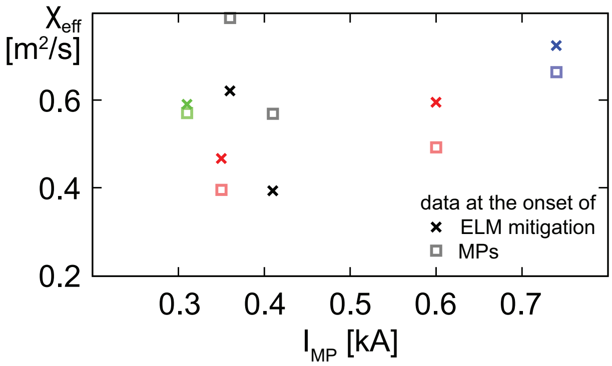


Figure 4: *Heat diffusivity at the onset of ELM mitigation (crosses) against the required MP-coil current for several discharges with different heating power and gas puff; the shaded squares indicate the corresponding values just before the MP onset.*

**Conclusion.** We demonstrated a reliable tool to investigate the effect of MPs on the edge kinetic data which enables us to resolve small differences in the edge pressure gradient threshold before type-I and mitigated ELMs. Generally, the occurrence of small ELMs is related to lower pedestal top temperatures and edge pressure gradients compared to type-I ELMs. The attainability of this parameter regime seems to be independent of the presence of MPs, but set by the amount of deuterium fuelling and heating power. The additional high-temperature small ELM regime in our high collisional plasma is unlikely to be caused by ergodization as proposed for the low collisionality DIII-D experiments [5] but might be related to a shifted stability threshold.

## References

[1] Suttrop W *et al* 2011 *Plasma Phys. Control. Fusion* **53** (12) 124014 and references therein
[2] Fischer R *et al* 2010 *Fusion Sci. Technol.* **58** (2) 675–684
[3] Rathgeber S K *et al* 2013 *Plasma Phys. Control. Fusion* **55** (2) 025004
[4] Suttrop W *et al* 1997 *Plasma Phys. Control. Fusion* **39** (12) 2051
[5] Evans T E *et al* 2004 *Phys. Rev. Lett.* **92** (23) 235003